Korean Journal of Chemical Engineering
https://doi.org/10.1007/s11814-024-00242-x

ORIGINAL ARTICLE

Assembly of ITO Nanocrystals into Nanotubes Using Polycarbonate Membranes for Dual-Band Electrochromic Modulation

Sungbin Kim[1] · Jungchul Noh[2] · Sungyeon Heo[1]

Received: 11 July 2024 / Revised: 22 July 2024 / Accepted: 23 July 2024

Abstract
Assembling doped metal oxide nanocrystals (NCs) into one-dimensional (1D) structures can enhance the optical and electrochemical properties of thin films. However, achieving this assembly without damaging the NCs' properties has been challenging. Here, we present facile method to assemble near-infrared (NIR) absorbing plasmonic indium tin oxide (ITO) NCs into 1D nanotubes (NTs) using track-etched polycarbonate (PC) membranes as templates. By infiltrating freestanding PC membranes with 3% doped ITO NCs, attaching them to an adhesive layer, and then annealing, we produce robust ITO NTs on substrates. Fabricated ITO NTs, featuring mesopores and macropores, exhibit rapid NIR modulation under electrochemical potential while maintaining static visible opacity, making them useful for privacy protection and thermal management. Incorporating NbO_x into these ITO NT films demonstrates rapid switching and electrochemically stable visible and NIR dual-band electrochromic modulation, highlighting the significance of structuring NCs.

Keywords Indium tin oxide · Polycarbonate membranes · Nanotubes · Nanocrystals · Electrochromic

Introduction

Doped metal oxide NCs exhibit excellent electronic properties and localized surface plasmon resonance (LSPR) absorption in the visible and infrared ranges, both originated from high charge carrier concentrations (10^{18}–10^{21} cm^{-3}) [1–4]. These properties can be dynamically adjusted through electrochemical charging and discharging, making them suitable for electrochromic applications [5–8]. Since both electrochemical and optical properties are influenced by thin film morphology, it is highly important to arrange them into desired structures [9, 10]. In NC electrochromic fields, the advanced functionalities such as transmittance control and fast electrochemical charging/discharging are achieved through assembling NCs [11–13].

Despite the significance of assembling NCs, aligning isotropic NCs in a specific direction poses challenges because isotropic NCs do not prefer oriented attachment. The assembly of NCs-polymer relies on chemical interaction between NCs and polymer moieties, demonstrating an efficient way to generate mesoporous structures from the structure-directing template agents [14–16]. However, 1D structuring through polymer–NCs interaction is particularly challenging due to the need of careful control of polymers, solvent, and NCs [17–19].

One of approach in directing NCs into the anisotropic structure involves arranging colloidal NCs using capillary force within spatial confinement [20]. Depending on the void shape, the morphology of the assembled NCs can mimic that of the void shape. Dong et al. demonstrated the successful assembly of Fe_2O_3 NCs into nanorods through capillary force using anodic aluminum oxide (AAO) membranes with 1D pores [21]. However, the method of inorganic template removal, which essentially relies on chemical etching such as strong KOH, is not suitable for chemically unstable materials like WO_3 and ITO NCs. These materials are crucial for electrochromic applications due to their absorption properties that match well with the solar spectrum. Therefore, alternative methods that do not degrade properties of the NCs are necessary.

✉ Sungyeon Heo
sungyeonh@seoultech.ac.kr

[1] Department of Chemical and Biomolecular Engineering, Seoul National University of Science & Technology, Seoul 01811, Republic of Korea

[2] McKetta Department of Chemical Engineering and Texas Material Institute, The University of Texas at Austin, Austin, TX 78712, USA

Published online: 31 July 2024

Main benefit of employing PC membranes as templates is their easy removal via thermal annealing or simple organic solvent dissolution, a method that cannot be applied to inorganic AAO membranes. This characteristic is especially advantageous for chemically unstable materials like WO_3 and ITO NCs, which are prone to damage from chemical etching. Earlier studies have investigated the incorporation of sol–gel-derived TiO_2, hydrothermal-grown ZnO, conducting polymers into the pores of PC membranes, aiming at applications in solar cells, actuator, and piezoelectric fields [22–25]. Nevertheless, there has been no investigation into assembling NCs into 1D structures using PC membranes and testing their electrochromic performance.

In this study, we first report assembly of shape isotropic ITO NCs into anisotropic 1D NTs using PC membranes as templates. NTs adhered to substrates via adhesion layer exhibit hollow structures that enhance electrolytes ion diffusion. The resulting films demonstrate NIR modulation when subjected to an electrochemical potential, with static opacity in the visible range. This holds promise for applications in privacy protection and thermal management. Moreover, the exterior void spaces of NTs and the hollow interior of the tubes play a crucial role in enabling dual-band electrochromic modulation with fast switching speeds when NbO_x is integrated. This underscores the importance of assembling NCs into 1D nanotubular structures for electrochemical applications.

Experimental Detail

Materials

ITO substrates (80 Ω/□) were purchased from Omniscience. Track-etched PC membranes (pore diameter = 200 nm, thickness ~ 10 μm) were obtained from Whatman Co. Niobium ethoxide ($Nb_2(OEt)_5$, 99.9%) was purchased from Alfa Aesar. Indium (III) acetate (99.99%), tin (IV) acetate, oleic acid, oleyl alcohol, dimethylformamide (DMF, ≥ 99.8%), hexane (≥ 95%), ethanol (≥ 99.5%), acetone (≥ 99.5%), nitrosyl tetrafluoroborate ($NOBF_4$), tetramethylammonium hydroxide ($NMe_4OH•5H_2O$, 97%), poly(vinyl chloride) (PVC, M_n = 62,000 g/mol), poly(oxyethylene methacrylate) (POEM, M_n = 500 g/mol), 1,1,4,7,10,10-hexamethyltriethylene tetramine (HMTETA, 99%), copper chloride (CuCl, 99%), N-methyl pyrrolidone (NMP, 99.5%), chloroplatinic acid solution (H_2PtCl_6), lithium perchlorate ($LiClO_4$, 99.99%) were purchased from Sigma-Aldrich. All solvents and chemicals were used as received.

ITO NC Synthesis

The ITO NCs were synthesized following a previously reported slow growth procedure [26]. Metal precursors of tin (IV) acetate and indium (III) acetate were dissolved in oleic acid and degassed under vacuum at 120 °C for 1 h. Desired doping concentrations were obtained by modifying the stoichiometric molar ratios of the precursors. Precursor solutions were then slowly injected (0.2 mL/min) into a reaction flask containing 12 mL of oleyl alcohol at 290 °C in inert condition. After the injection, the flask was cooled to room temperature, and the NCs were precipitated with ethanol, centrifuged at 8500 rpm for 5 min and then precipitate was dispersed in hexanes. The washing procedure was repeated two more times.

Ligand Stripping of ITO NCs

To remove the ligands from the NC surfaces, $NOBF_4$ salts were used [27]. Purified ITO NCs dispersed in hexane were combined with DMF to form a biphasic mixture, with the non-polar phase on top. $NOBF_4$ was then added to this mixture in a 1:1 weight ratio with the ITO NCs, and the mixture was stirred for 1 h. Once the stripping reaction was successfully completed, the NCs were transferred to the polar DMF phase. The stripped NCs were then purified by centrifugation using DMF and toluene as the solvent/anti-solvent pair.

Synthesis of PVC-*g*-POEM Graft Copolymer

Poly(vinyl chloride)-*g*-poly(oxyethylene methacrylate) (PVC-*g*-POEM) graft copolymers were synthesized by atom transfer radical polymerization (ATRP) [28]. 6 g of PVC was dissolved in 50 mL of NMP by stirring at room temperature until PVC was fully dissolved. After this procedure, 27 g of POEM, 0.1 g of CuCl, and 0.24 mL of HMTETA were added to the solution. The green mixture was stirred until a homogeneous solution was obtained and then purged with nitrogen for 1 h. The reaction was carried out at 90 ℃ for 24 h. After polymerization, the solution was precipitated with methanol three times. PVC-*g*-POEM graft copolymer was obtained and dried in a vacuum oven overnight at 50 ℃.

Preparation of ITO NTs Film

PC membranes underwent pretreatment process where they were immersed in hexane for 20 min, dried, and then re-immersed for 20 min in ITO NCs solution dispersed in hexane at a concentration of 75 mg/mL. The attachment of PC membrane to the ITO-coated glasses was achieved by introducing a nanocomposite adhesive layer composed of

PVC-*g*-POEM and ligand-stripped 0.1%-doped ITO NCs. The solution for the adhesive layer was prepared as follows: first, 0.11 g of PVC-*g*-POEM was dissolved in 3 mL of DMF, followed by the addition of 1.5 mL of ligand-stripped ITO solution (80 mg/mL). This solution was spin-coated onto the ITO substrates at 1500 rpm for 30 s. Before the adhesive layer dried completely, PC membrane infiltrated with NCs was attached to it. The samples were then annealed at 500 °C for 2 h to remove the templates.

Preparation of ITO NTs/NbO_x Composite Film

Niobium polyoxometalate (Nb-POM) clusters were synthesized by following a previous report [29]. A solution was prepared by dissolving 140 mg of N b_{10} POM in 1 mL of ethanol/deionized water mixture (1:1 volume ratio). The POM concentration was delicately adjusted to prevent forming an overlayer on the surface of the NTs film. 50 µL of the solution was drop-casted onto the fabricated ITO NTs film, which was then ramped to 4000 rpm, and spun for 1 min. Subsequently, the film was annealed in air at 400 °C for 30 min to condensate the POMs.

Preparation of ITO NC Densely Packed Film

To fabricate the same form of ITO NTs film, adhesion layer was spin-coated on the ITO-coated glasses. The film was then annealed at 500 °C for 2 h to remove the polymer templates. After annealing, ITO solution (120 mg/mL) was spin-coated with 1500 rpm for 1 min. To achieve similar thickness to ITO NTs film, the film was treated with formic acid and then spin-coated with the ITO solution in the same manner as before. This process was repeated to achieve the similar thickness of the ITO NTs film.

FTIR Measurement

The transmittance spectra of PVC-*g*-POEM were recorded on a Nicolet iS50 FTIR spectrometer. Each solution was dropped on a double side polished Si wafer and dried.

Scanning Electron Microscopy (SEM) and Transmission Electron Microscopy (TEM) Measurements

SEM and TEM images were measured by a Hitachi SU8010 and a JEOL JEM-2010, respectively. Samples for SEM measurement were prepared on silicon wafers. TEM measurement samples were prepared by drying a drop of solution on the copper TEM grids with lacey carbon support films (300 mesh, Sigma-Aldrich).

UV–Visible–NIR Spectra Measurement

The absorbance spectra of ITO NCs with varying tin doping concentrations, dispersed in tetrachloroethylene, were recorded using a JASCO V-770 UV–VisNIR spectrophotometer.

In Situ Spectroelectrochemical Measurement

A home-built in situ spectroelectrochemical cell was installed in an argon glovebox. Visible and NIR transmission spectra of ITO thin films were obtained in situ using Oceanview 2.0 software. The samples deposited on ITO substrates were positioned as the working electrode in a two-electrode system. A Li foil was used as the counter and reference electrode. 0.1 M $LiClO_4$ in propylene carbonate (PC) was used as the electrolyte. Chronoamperometry (CA) was conducted to measure film's optical property in the visible and NIR region. Cyclic voltammetry (CV) is used to measure cycling stability between 1.5 and 4 V (vs Li/Li^+) with the sweep rates (40 mV/sec for ITO NTs, ITO NTs/NbO_x composite film).

Results and Discussion

First, PC membranes with pore diameter of 200 nm were selected to fabricate 1D ITO NTs. To dynamically modulate NIR transmittance which are crucial for thermal management, 10 nm-sized-3%-doped ITO NCs shown in Fig. 1c were synthesized to minimize NIR absorption at the bleached states while maximizing NIR modulation at the colored state. Thus, as-synthesized ITO NCs absorption is low in 300–1600 nm while strong absorption around 2000 nm wavelength (Fig. 1a). It should be mentioned that the NCs are dispersed in the hexane to protect membranes as PC membranes are quickly dissolved in the toluene solvent. PC membranes were dipped into the 3%-doped ITO NCs solution for capillary force induced infiltration (Scheme 1). After films were taken out, the surface of the PC membranes was gently wiped out to remove the redundant ITO NCs. Otherwise, an additional layer of ITO NC film would form after the annealing process (Fig. S1).

Due to the freestanding nature of PC membranes, adhesive layers are crucial for fabricating robust ITO NT films on substrates. The adhesive layer consists of the assemblies of PVC-*g*-POEM and ITO NCs, with POEM providing the adhesive properties. 0.1%-doped ITO NCs with 13 nm size were chosen to minimize modulation in the NIR range (Fig. 1a, b). Agrawal et al. showed that low-doped, large-sized ITO NCs exhibit minimal modulation due to the surface depletion effect [30]. This approach minimizes the convolution effect to NIR modulation during electrochemical

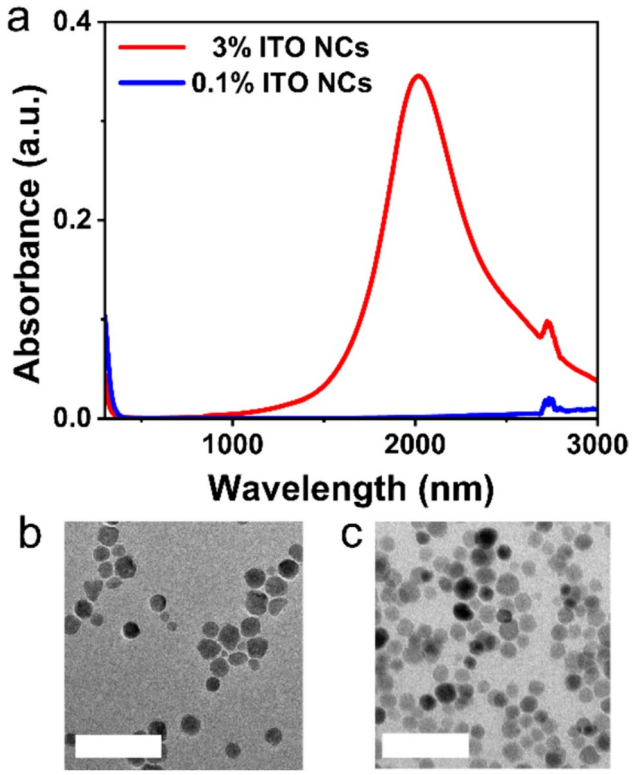

Fig. 1 **a** Absorbance spectra of 3%-doped and 0.1%-doped ITO NCs dispersed in the tetrachloroethylene and TEM images of **b** 0.1%-doped (left) and **c** 3%-doped (right) ITO NCs (scale bar: 50 nm)

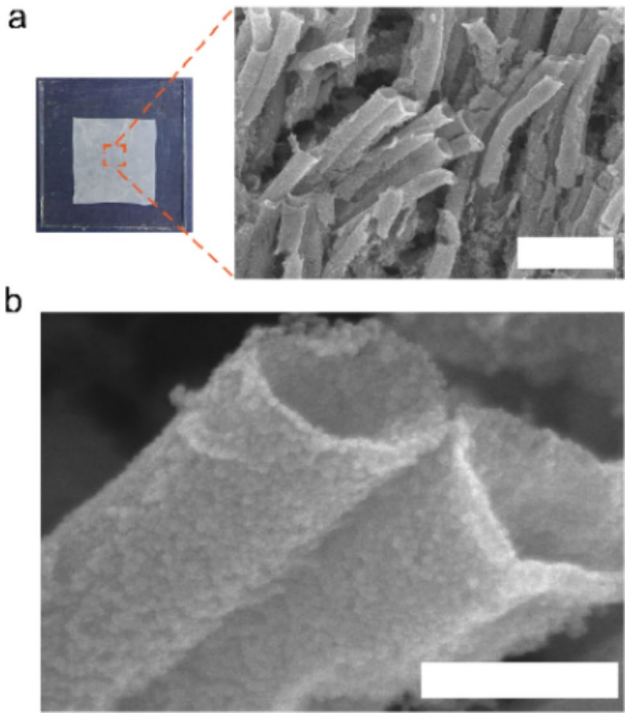

Fig. 2 **A** Optical image of 3%-doped ITO NTs on the ITO substrate and a SEM image of the 3%-doped ITO NTs at a concentration of 75 mg/ml (scale bar: 1 μm), **b** A SEM image of ITO NTs showing the pore existence (scale bar: 200 nm)

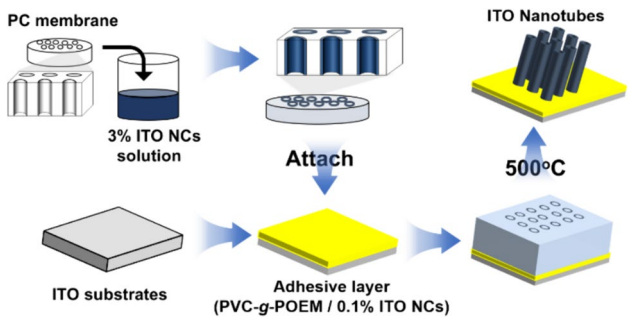

Scheme 1 Schematic illustration for fabrication of ITO NTs using PC membranes

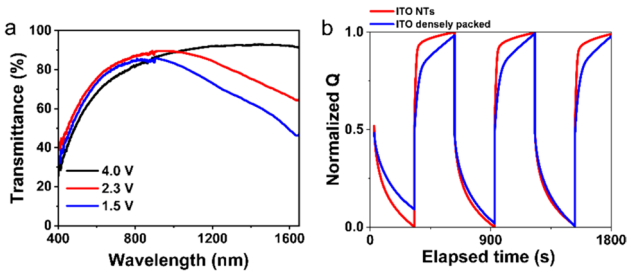

Fig. 3 **a** In situ transmittance spectra of 3%-doped ITO NTs with 0.1%-doped ITO NCs bottom layer that formed after the annealing at different applied potential, **b** normalized charging and discharging profiles following potential step (1.5 V, 4 V)

test. The synthesized 0.1%-doped ITO NCs were ligand-stripped to enable assembly with PVC-*g*-POEM synthesized by atom transfer radical polymerization technique (Fig. S2) [28, 31]. When the ITO NC volume ratio increases, the POEM ratio decreases in the deposited film, reducing adhesive property with PC membranes (Fig. S3). The PVC-*g*-POEM and 0.1%-doped ITO NCs (80 mg/ml) mixed solution was spin-coated onto ITO substrates. PC membranes infiltrated with NCs were immediately attached to the adhesive layer and annealed in air at 500 °C to remove PC membranes and PVC-*g*-POEM templates. It should be noted that the PC membrane template removal process is not considered as an additional step, since thermal annealing is necessary to remove the ligands from the ITO NCs.

As shown in Fig. 2a, the annealed films show the successful fabrication of ITO NTs on the substrates. Figure 2b demonstrates the presence of ITO NCs, indicating the existence of mesopores formed by the packing of these NCs, alongside macropores within the NTs. The optical image shows opacity in the visible range while maintaining transparency in the NIR range (Fig. 2a and Fig. 3a). The opacity with low transmittance

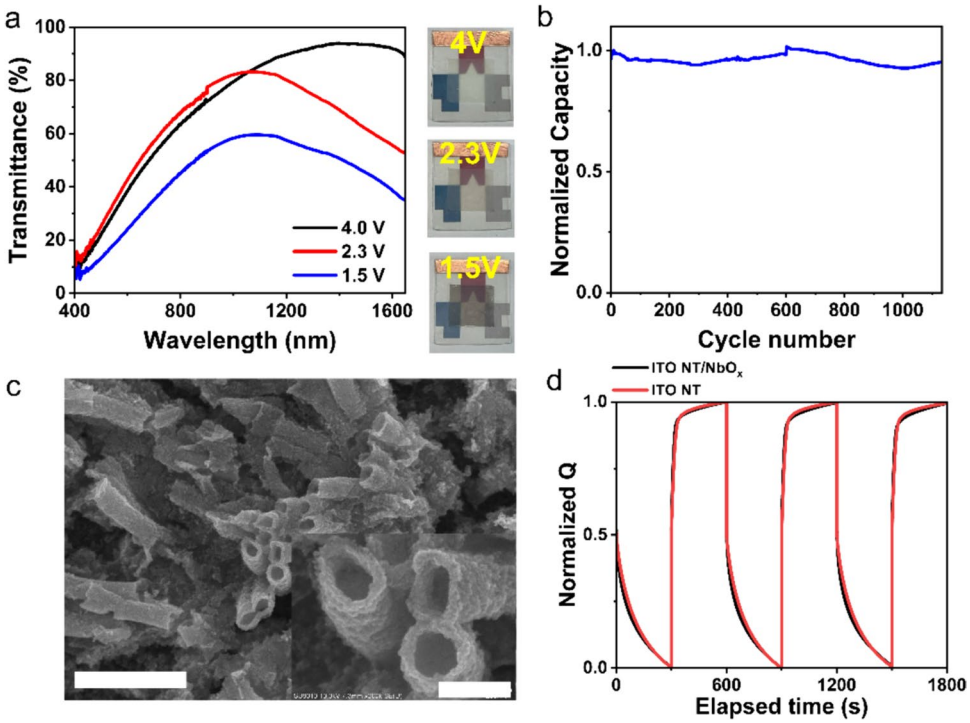

Fig. 4 **A** Transmittance spectra and corresponding photographs of ITO NTs/NbO_x composite films on ITO substrate at each potential, **b** normalized charge capacity of ITO NTs/NbO_x composite films. Samples were cycled by cyclic voltammetry method between 1.5 and 4 V, **c** SEM images of the ITO NTs/NbO_x composites (scale bar: 1 µm). Inset shows pore existence in the composite films (scale bar: 200 nm), **d** normalized charging and discharging profiles following potential step (4 V, 1.5 V)

in the visible range (400—800 nm) is due to the micrometer-sized nanotubular structure, contributing to the enhanced light scattering effect. When the concentration of the 3%-doped ITO NCs solution gradually increases, the length of the NTs also increases (Fig. S4) while preserving nanotubular structure. The presence of hollow structure is expected to facilitate electrolytes ion diffusion during the electrochemical modulation.

The electrochromic properties of ITO NTs film were evaluated with an in situ spectroelectrochemical setup in a glovebox. At 4 V (vs Li/Li^+), the film exhibited low transmission in the visible spectrum due to the significant scattering effect, but high transmission in the NIR range owing to the negligible absorption from the low doping level (3%) of ITO NCs (Fig. 3a). When the potential decreases to 1.5 V, the NIR transmittance decreased from enhanced LSPR absorption from the electrochemical charging effect while the visible transmittance slightly increased. It should be mentioned that the modulation in Fig. 3a is primarily from the 3%-doped ITO NTs with minimal contribution from the bottom 0.1%-doped ITO NCs layer (Fig. S5). The static visible opacity combined with NIR modulation properties of these films can be applied for privacy protection and thermal management purposes. The presence of mesopores and macropores resulting from NC packing, along with void spaces within the nanotubular structure, is anticipated to improve the electrochemical switching speed. In comparison to densely packed 3%-doped ITO NC films of similar thickness, ITO NT films show fast electrochemical switching capabilities (Fig. 3b).

These highly porous films offer opportunities for incorporating external components. In our electrochromic application, we introduced niobium polyoxometalate (POM) clusters $[Nb_{10}O_{28}]^{6-}$ via spin coating, followed by thermal condensation to form NbO_x [29]. NbO_x is known to induce visible modulation through polaronic absorption mechanisms. To optimize the concentration of Nb-POM, various concentrations were tested. Compared to the 120 mg/ml Nb-POM concentration depicted in Fig. S6, a solution with 140 mg/ml of Nb-POM (Fig. 3a) resulted in increased modulation in the NIR range due to the slightly higher concentration of Nb-POM. However, introducing 160 mg/ml of Nb-POM decreased the modulation (Fig. S6). Therefore, we chose a concentration of 140 mg/ml of Nb-POM for further spectroelectrochemical studies.

The in situ electrochromic performance of the ITO NTs/NbO_x composite film was evaluated by applying different potentials (4 V, 2.3 V, 1.5 V), resulting in independent dual-band modulation in the visible and NIR range (Fig. 4a). At 4 V, the composite film exhibits visible opacity while maintaining NIR transparency. Applying 2.3 V induces NIR modulation due to capacitive charging while maintaining visible opacity. When reduced to 1.5 V, the film turned into the darkish color in the visible range and further blocked NIR light. Notably, the switching speed of the ITO NTs/NbO_x film is similar to that of only ITO NTs film (Fig. 4d), probably attributed to efficient ion diffusion across the ITO/NbO_x/electrolyte interfaces (ITO ↔ NbO_x, NbO_x ↔ electrolytes, ITO ↔ electrolytes), as previously discussed by Kim et al. [11]. Moreover, as can be seen from Fig. 4c, there are still pores inside the tubes, and expected to contribute fast switching speed. When a dense ITO NCs film is coated

with Nb-POM at a concentration of 120 mg/ml, the film is clearly covered with Nb-POM (Fig. S7), highlighting the significance of NCs structuring. Moreover, compared to ITO NT films prone to rapid electrochemical degradation (Fig. S8), the ITO NTs/NbO_x composite films exhibit sustained electrochemical cycling stability, possibly attributed to the adhesive role of the NbO_x layer in preventing delamination of ITO NCs (Fig. 4b) [11, 29].

Conclusion

In summary, we demonstrated an efficient method to assemble shape isotropic ITO NCs into anisotropic 1D NT structures using PC membranes that have 1D pores. The ITO NTs are fabricated on ITO substrates with the help of PVC-g-POEM/ ITO adhesive layer, followed by thermal annealing to remove the organic templates. The PC membranes were easily removed through thermal annealing, which is an essential step for removing ligands from the ITO NCs. Further infiltration of Nb-POM followed by thermal condensation process gives visible and NIR dual-band modulation under applied potential, leveraging the open porous network of 1D NTs. For scaling up to larger electrochromic devices, future development of PC membranes with higher pore density and larger dimensions will be necessary. Our study suggests that thermally or solvent removable PC membranes hold promise as templates for assembling inorganic NCs into 1D structures, applicable across various fields.

Supplementary Information The online version contains supplementary material available at https://doi.org/10.1007/s11814-024-00242-x.

Acknowledgements This study was supported by the Research Program funded by the SeoulTech (Seoul National University of Science and Technology).

Data availability The data will be available from the corresponding author upon request.

Declarations

Conflict of Interest There are no conflicts to declare.

References

1. E.L. Runnerstrom, A. Llordés, S.D. Lounis, D.J. Milliron, Chem. Commun. **50**, 10555 (2014)
2. J. Van Embden, S. Gross, K.R. Kittilstved, E. Della Gaspera, Chem. Rev. **123**, 271–326 (2023)
3. B. Tandon, S.L. Gibbs, B.Z. Zydlewski, D.J. Milliron, Chem. Mater. **33**, 6955–6964 (2021)
4. X. Liu, M.T. Swihart, Chem. Soc. Rev. **43**, 3908–3920 (2014)
5. K. Wang, Q. Meng, Q. Wang, W. Zhang, J. Guo, S. Cao, A.Y. Elezzabi, W.W. Yu, L. Liu, H. Li, Adv. Energy Sustain. Res. **2**, 2100117 (2021)
6. S. Cao, S. Zhang, T. Zhang, Q. Yao, J.Y. Lee, Joule **3**, 1152–1162 (2019)
7. S. Heo, J. Kim, G.K. Ong, D.J. Milliron, Nano Lett. **17**, 5756–5761 (2017)
8. J. Fortunato, B.Z. Zydlewski, M. Lei, N.P. Holzapfel, M. Chagnot, J.B. Mitchell, H.-C. Lu, D. Jiang, D.J. Milliron, V. Augustyn, ACS Photonics **10**, 3409–3418 (2023)
9. J. Zimou, K. Nouneh, R. Hsissou, A. El-Habib, L.E. Gana, A. Talbi, M. Beraich, N. Lotfi, M. Addou, Mater. Sci. Semicond. Process. **135**, 106049 (2021)
10. B. Tandon, A. Agrawal, S. Heo, D.J. Milliron, Nano Lett. **19**, 2012–2019 (2019)
11. J. Kim, G.K. Ong, Y. Wang, G. LeBlanc, T.E. Williams, T.M. Mattox, B.A. Helms, D.J. Milliron, Nano Lett. **15**, 5574–5579 (2015)
12. H. Jiang, B. Zhu, Z. Qi, Y. Xue, S. Cao, Appl. Surf. Sci. **611**, 155711 (2023)
13. S. Cao, S. Zhang, T. Zhang, J.Y. Lee, Chem. Mater. **30**, 4838–4846 (2018)
14. G. Manai, H. Houimel, M. Rigoulet, A. Gillet, P.-F. Fazzini, A. Ibarra, S. Balor, P. Roblin, J. Esvan, Y. Coppel, B. Chaudret, C. Bonduelle, S. Tricard, Nat. Commun. **11**, 2051 (2020)
15. P. Innocenzi, L. Malfatti, G.J.A.A. Soler-Illia, Chem. Mater. **23**, 2501–2509 (2011)
16. M.R.J. Scherer, U. Steiner, Nano Lett. **13**, 3005–3010 (2013)
17. P. Pula, A.A. Leniart, J. Krol, M.T. Gorzkowski, M.C. Suster, P. Wrobel, A. Lewera, P.W. Majewski, A.C.S. Appl, Mater. Interfaces **15**, 57970–57980 (2023)
18. A. Berg, H. Jonkman, K. Loos, G. Portale, B. Noheda, A.C.S. Appl, Nano Mater. **5**, 13349–13360 (2022)
19. A. Horechyy, J. Paturej, B. Nandan, D. Jehnichen, M. Göbel, U. Reuter, J.-U. Sommer, M. Stamm, J. Colloid Interface Sci. **578**, 441–451 (2020)
20. J. Feng, Y. Qiu, H. Gao, Y. Wu, Acc. Chem. Res. **57**, 222–233 (2024)
21. S. Wan, X. Xi, H. Zhang, J. Ning, Z. Zheng, Z. Zhang, Y. Long, Y. Deng, P. Fan, D. Yang, T. Li, A. Dong, ACS Nano **16**, 21315–21323 (2022)
22. S.Y. Heo, D.J. Kim, H. Jeon, B. Jung, Y.S. Kang, J.H. Kim, RSC Adv. **3**, 13681–13684 (2013)
23. S. Stassi, V. Cauda, C. Ottone, A. Chiodoni, C.F. Pirri, G. Canavese, Nano Energy **13**, 474–481 (2015)
24. P. Chen, X. Shang, T. Hang, Nano Lett. **24**, 1423–1430 (2024)
25. D.K. Roh, R. Patel, S.H. Ahn, D.J. Kim, J.H. Kim, Nanoscale **3**, 4162–4169 (2011)
26. A.W. Jansons, J.E. Hutchison, ACS Nano **10**, 6942–6951 (2016)
27. A. Dong, X. Ye, J. Chen, Y. Kang, T. Gordon, J.M. Kikkawa, C.B. Murray, J. Am. Chem. Soc. **133**, 998–1006 (2011)
28. D.K. Roh, J.T. Park, S.H. Ahn, H. Ahn, D.Y. Ryu, J.H. Kim, Electrochim. Acta **55**, 4976–4981 (2010)
29. A. Llordés, G. Garcia, J. Gazquez, D.J. Milliron, Nature **500**, 323–326 (2013)
30. O. Zandi, A. Agrawal, A.B. Shearer, L.C. Reimnitz, C.J. Dahlman, C.M. Staller, D.J. Milliron, Nat. Mater. **17**, 710–717 (2018)
31. D.H. Kim, M.S. Park, Y. Choi, K.B. Lee, J.H. Kim, J. Chem. Eng. **346**, 739–747 (2018)